SKIN AND STRUCTURAL TEMPERATURE MEASUREMENTS ON RESEARCH AIRPLANES AT SUPERSONIC SPEEDS

By Richard D. Banner and Frank S. Malvestuto, Jr.

NACA High-Speed Flight Station

INTRODUCTION

The NACA High-Speed Flight Station is presently engaged in a comprehensive program to investigate and analyze the aerodynamic heating of airplanes in flight at supersonic speeds. Skin and structural temperatures have been determined in flight by use of thermocouples and temperature resistance gages installed on various research airplanes. Such data have recently been obtained on two research airplanes, the Bell X-2 and the Bell X-1B. The object of this paper is to show some of the actual magnitudes and trends in the structural temperatures that exist in an airplane experiencing the effects of aerodynamic heating. Although time has not permitted an analysis of much of these temperature data, the information presented herein is a cross section of the work that is presently being done. The data presented do not cover the speed and altitude range anticipated for the proposed North American X-15; however, they provide actual full-scale, experimental, structural temperature information for comparison with present analytical and wind-tunnel studies.

Shown in figure 1 is a sketch of the two airplanes. The X-2 airplane is constructed primarily of steel. Nose-cone skin temperatures have been obtained on this airplane at supersonic speeds up to a Mach number of 3.2. The X-1B airplane is constructed primarily of aluminum. The maximum speed capability of the X-1B is less than that of the X-2. Very extensive temperature measurements are being made throughout the structure of the airplane. To date, data have been obtained in flight to a Mach number of 1.8 at about 300 locations throughout the airplane.

DATA OBTAINED ON THE BELL X-2 AIRPLANE

Data were obtained on the Bell X-2 nose cone at flight conditions shown in figure 2. The Mach number is shown for only the supersonic portion of the flight. The maximum Mach number of 3.2 was reached at an altitude of 62,000 feet about 160 seconds after drop. The air temperature at this altitude and down to the altitude for drop was approximately -90° F. The structure prior to drop was only slightly warmer. The angles of attack for the flight conditions shown were small.

As mentioned previously, only nose-cone skin temperatures were measured on the X-2. Figure 3 shows, in time-history form, the measured skin temperatures at stations 9.5 and 35.25 inches back of the nose-cone apex. Maximum temperatures on the order of 420° to 430° F were measured at the two stations shown. (It should be pointed out here that all the skin temperatures were measured on the inside surface of the skin.) The theoretical stagnation temperature, which is shown as the upper curve, reads a maximum of 700° F at a Mach number of 3.2. The turbulent adiabatic, or insulated, wall temperature was estimated by using a recovery factor of 0.9 and is shown as the second curve from the top. The maximum adiabatic wall temperature was 630° F. The difference between the adiabatic wall temperature and the skin temperature shown here is due, of course, to the conductivity of the skin. The temperature of the nose-cone compartment was measured during the flight and is shown as the lower curve. The measuring point for the compartment temperature was $1\frac{1}{2}$ inches from the skin. A maximum nose-cone-compartment temperature of about 60° F was measured. A spot check indicated that this temperature was due primarily to the effects of the skin's internal radiation.

Time-history data at several points along the nose cone are briefly summarized in figure 4 which shows the longitudinal temperature distribution at three times during the flight. The data are shown at Mach numbers of 1.4, 3.20 (the maximum Mach number), and 9 seconds later at a Mach number of 3.00. At a Mach number of 1.4, the temperatures were constant along the cone at a little above 0°. At the higher speeds and higher temperatures, there are some inflections in the curves shown. These inflections are associated with the heat sinks in the regions of the internal bulkheads. It should be pointed out that the skin thicknesses at the locations shown in this figure were constant at 0.019 inch. Some effects of material thickness can be seen in figure 5, which shows time histories of the temperatures measured on the top and bottom of the nose cone. The stations for which these temperature data are shown are 9.5 and 18.44 inches back of the nose-cone apex. The temperatures measured on top are shown by the solid lines. The material thickness on the top is 0.019 inch. The dashed lines are the bottom temperatures, measured on the inside of a splice plate. The total thickness on the bottom, including splice, is 0.038 inch. The skin temperatures on top of the nose cone, at both stations, reached a maximum of about 400° F at approximately the same time. The bottom temperatures, measured on the splice plate, lagged the top, as might be expected from the conductivity effect of the increased thickness. Also, the effectiveness of the welded splice joint no doubt affects the temperatures indicated on the bottom.

Measured data have been presented for various conditions on the X-2 nose cone during flight at angles of attack near zero. It was noticed that only small differences in the maximum skin temperatures existed

at the locations where conduction effects to the internal structure were negligible. It is of interest to compare these measured temperatures with those calculated by theory. Figure 6 shows a time-history comparison of the measured and calculated temperatures at two locations on the side of the X-2 nose cone. The measured data are shown by the solid curves. The calculations, which are based on the Colburn relationship for a turbulent boundary layer on a flat plate and modified to a cone, are shown as dashed lines. As can be seen, the calculations give a 20- to 25-percent conservative estimate of the skin temperatures. A check at several points indicated that use of Van Driest's turbulent theory would have given estimates of the skin temperatures about 10 to 15 percent lower than the calculations used here. The local Reynolds numbers used in the calculations were based on the distance rearward of station 0, as shown in the sketch. It should be pointed out that the X-2 has a nose boom (which is not shown completely in figure 6) that protrudes about 3 feet ahead of the nose cone. Wind-tunnel studies have indicated that such protuberances are very effective in producing turbulent flow. The existence of a turbulent boundary layer at these stations can be seen in the comparison of the calculated and measured-skin-temperature data.

DATA OBTAINED ON THE BELL X-1B AIRPLANE

As pointed out previously, very extensive temperature measurements are being obtained on the Bell X-1B airplane. These measurements include not only the skin temperatures on the wing and tail surfaces but also the temperatures on the spars and supporting structure where the internal heat conduction effects are greatest. Fuselage skin temperatures are also being measured and an attempt is being made to assess the effects on the structural temperatures of the internal heat sinks and sources, such as the fuel and liquid-oxygen tanks and the rocket engine.

Presented in figure 7 are the supersonic flight conditions for the X-1B airplane. The altitude varied between 50 and 58,000 feet and the ambient air temperature was approximately -90° F at the altitudes shown. The angles of attack during flight were small and varied between 0° and 4°.

The ambient air temperature is shown in figure 7 in order to give an indication of the temperature of the X-1B prior to drop. The structure of the airplane was approximately 10° to 20° warmer than the ambient air temperature. In the region near the liquid-oxygen tank, however, the temperatures were considerably colder.

Figure 8 shows the longitudinal variation of temperatures measured on the fuselage at a Mach number of 1.6, during the accelerating portion of the flight, and at a Mach number of 1.8, the maximum Mach number for

the flight. The temperatures are given for the locations shown by the black dots along the fuselage. The skin thicknesses at these locations are indicated above. The theoretical stagnation temperature at a Mach number of 1.8 is 150° F.

In the stagnation region of the nose, temperatures on the order of 110° to 115° were measured. The temperatures decrease slightly at positions rearward along the fuselage to a point on the side of the cockpit. The skin thicknesses in this region differ only slightly. The next point shown, however, is in the region of the liquid-oxygen tank, where the skin thickness is increased considerably. The temperature in this region drops rapidly to about -25° F.

In the fuselage region just above the wing, the material thickness increases slightly and the temperatures decrease to about 50°. At the next location shown, where the thickness is 0.072 inch, the skin temperature is also about 50° F. The temperatures increase at positions rearward along the fuselage to about 75° in the very rear portion. It can be seen that in this region the skin thicknesses have decreased and are of the same order as those near the nose. Heat sources, such as the rocket engine, and heat sinks, such as the liquid-oxygen and fuel tanks, affect the skin temperatures shown; however, it is felt that these variations in the fuselage skin temperatures are typical of those that would be encountered on research airplanes.

Temperature distributions for two fuselage cross sections and along the chord of the vertical tail at a midspan station are shown in figure 9. The data are again shown for the following flight conditions: a Mach number of 1.8, a stagnation temperature of 150° F, and an ambient air temperature of -90° F.

On the nose station of the fuselage the temperatures measured around the periphery are about constant at 90° F. The material thickness here is also constant.

At the aft fuselage station, the temperatures gradually decrease from about 80° F on the side of the vertical tail down to about 60° F near the bottom of the fuselage. There is a small inflection in the temperatures near the intersection of the vertical tail and the horizontal tail. This decrease in temperature is partly due to the increased material thickness in this particular area.

The chordwise variations of the vertical-tail skin temperatures are shown at the bottom of figure 9. The temperatures decrease with increasing distance along the chord, from a value of about 100° F at the leading edge. The slight increase in the temperature near the trailing edge is due to the decreased skin thickness on the rudder.

The temperatures shown by the black squares were measured on the center line of the vertical-tail spars. The difference between these temperatures and the skin temperatures is seen to be about 30° F.

In figure 10 are shown the chordwise temperature variations measured on the wing at the 54-percent semispan station and the 95-percent semispan station (or a tip station). The thermocouple locations are indicated by the black dots. The skin thicknesses vary from front to rear at both span stations. For the upper surface of the inboard station, these thicknesses are 0.081 inch at the leading edge, 0.270 inch in the wing box section, and 0.064 inch on the flap. For the lower surface of the inboard station they are 0.081 inch, 0.230 inch, and 0.064 inch. Skin thicknesses at the tip station along the upper and lower surfaces vary from 0.064 inch to 0.072 inch and again to 0.064 inch on the aileron. The wing is of multiple-spar construction, the spars serving as internal heat sinks. For this reason, the data are not faired continuously along the chord.

The chordwise temperatures at the 54-percent-semispan station may be seen to decrease from the leading edge back along the chord to the forward end of the flap and then increase near the trailing edge. Theoretical estimates of these temperature variations have not been completed; however, the variations are understandable. The decrease in the aerodynamic heat input with increasing distance from the leading edge results in lower temperatures. Of course, the change in skin thickness along the chord has a considerable influence on the temperatures; for example, the thinner skin in the trailing-edge region accounts for the increase of skin temperature in this region. Also, the temperatures in the center section are, relatively speaking, very low due to the increased skin thickness in this region. The general level of the temperatures at the tip region is higher than at the inboard station. Apparently, the increased level is associated with the thinner skins at this span station. It is realized, however, that aerodynamic input in the tip region is not the same as the input at the midsemispan station.

In order to give some indication of the internal-conduction effects in the wings of research airplanes, time histories of the temperatures that were measured on and near the spars at the 54-percent semispan station are shown in figure 11. The left sketch shows the temperatures measured in the leading-edge region. The temperature of the leading edge, as shown in figure 10, is a maximum of about 90° F. The internal temperatures on the relatively thick spar and the spar flanges are seen to be considerably lower.

The data for all the spar locations show, as would be expected, that the temperatures at the spar center line are lower than the temperatures of the upper and lower skins. This trend seems to be true also at the leading edge of the flap where not only conduction but also convection effects influence the temperature.

The spanwise variation of the wing skin temperatures is shown in figure 12. Shown above the wing are the temperatures that were experienced on the leading edge, and also on the upper skin at the 66-percent-chord station. As can be seen, the leading-edge temperatures vary from about 90° F near the root to a little above 100° F near the tip. The skin temperatures at the 66-percent-chord station are lower, particularly at the root where the wing skin thickness is 0.5 inch. The spanwise variation in the skin thickness is shown below for both the 66-percent-chord station and the leading edge. It is interesting to note that the temperature variations over the span are roughly proportional to the inverse of the skin thickness. The existence of these trends at higher temperature levels may result in important thermoelastic effects, particularly in the wing-tip region.

RESEARCH AIRPLANES UTILIZED FOR TEMPERATURE STUDIES

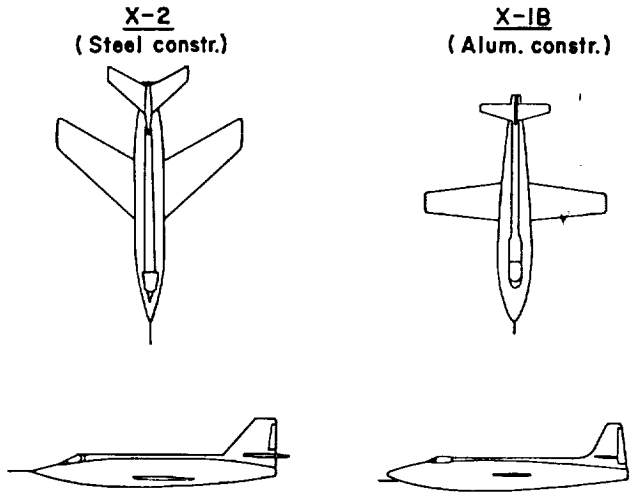

Figure 1

X-2 AIRPLANE—FLIGHT CONDITIONS

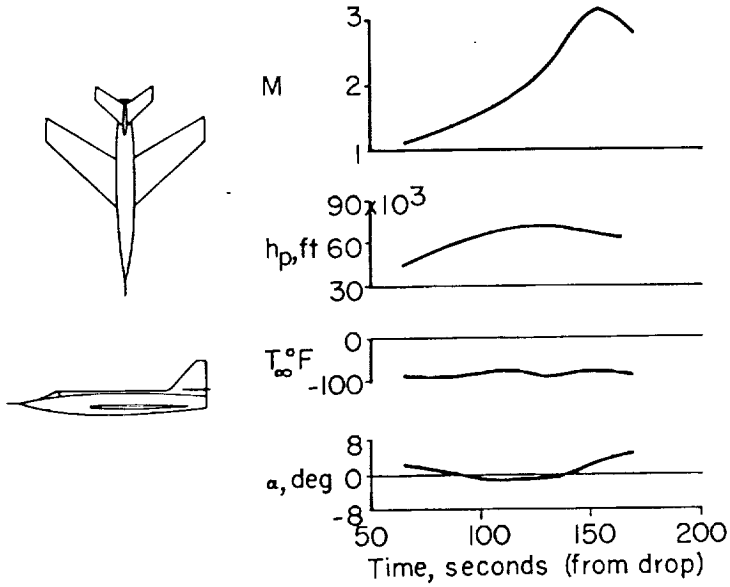

Figure 2

TIME HISTORY OF SKIN TEMPERATURES — X-2 NOSE CONE

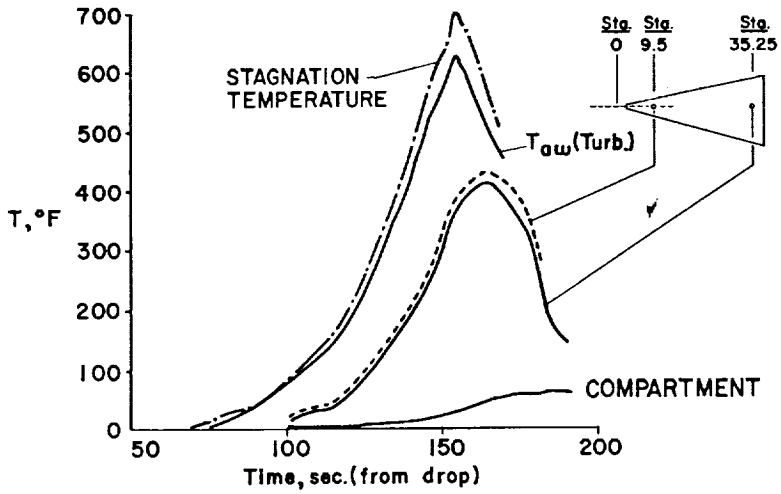

Figure 3

LONGITUDINAL SKIN TEMPERATURE DISTRIBUTIONS X-2 NOSE CONE

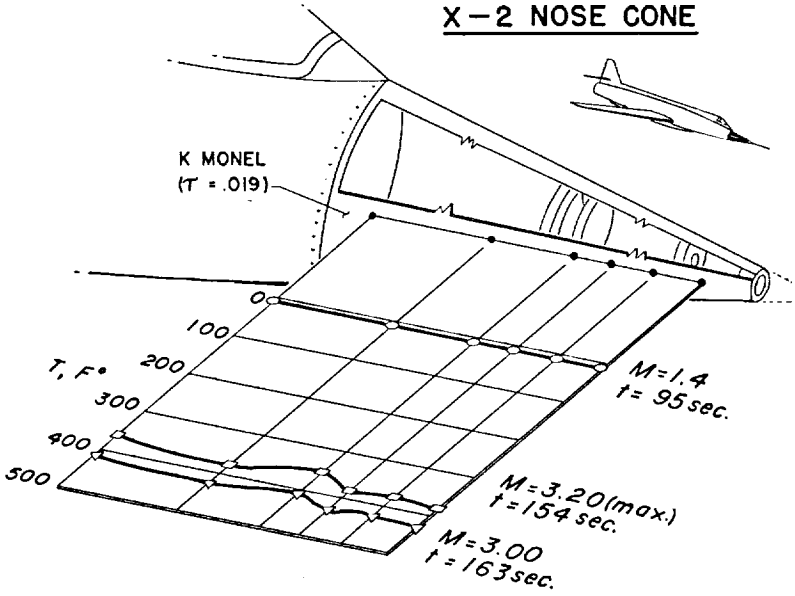

Figure 4

TIME HISTORY OF SKIN TEMPERATURES — TOP AND BOTTOM OF X-2 NOSE CONE

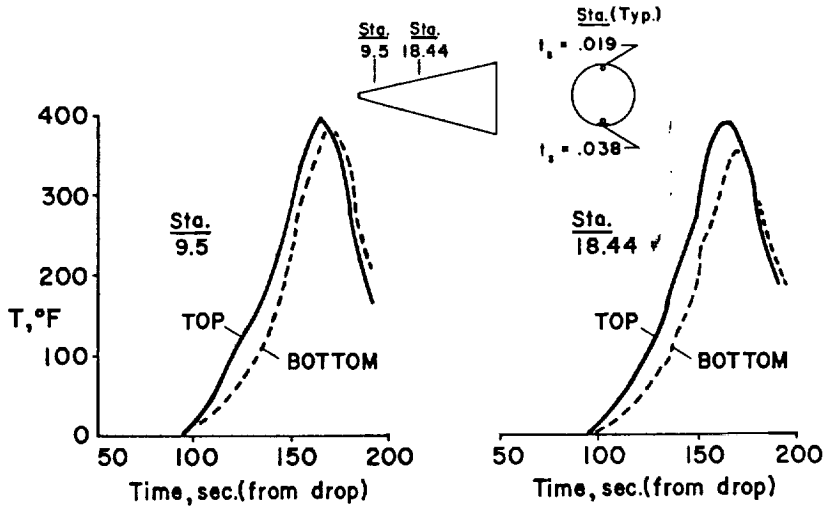

Figure 5

MEASURED AND CALCULATED SKIN TEMPERATURES—X-2 NOSE CONE

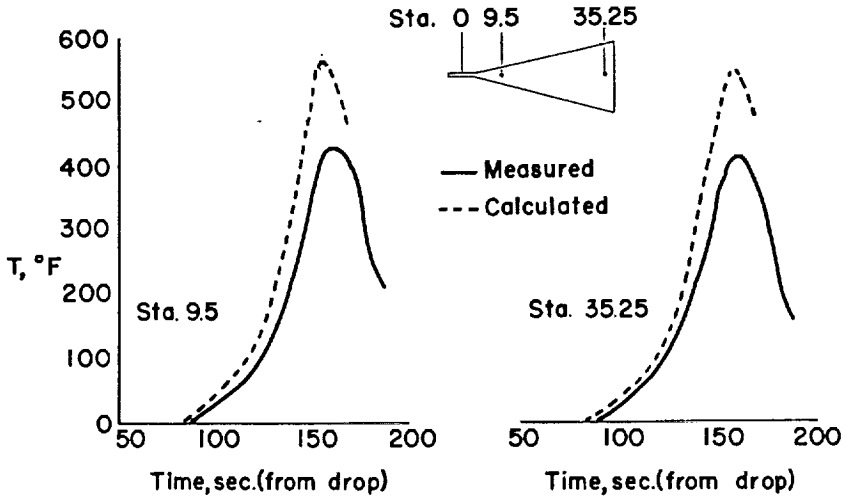

Figure 6

X-1B AIRPLANE—FLIGHT CONDITIONS

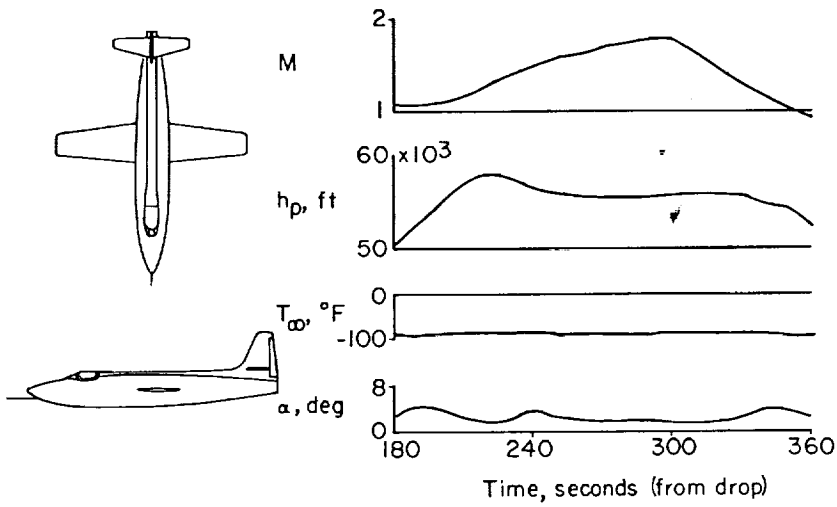

Figure 7

LONGITUDINAL SKIN TEMPERATURE DISTRIBUTIONS
X-1B FUSELAGE

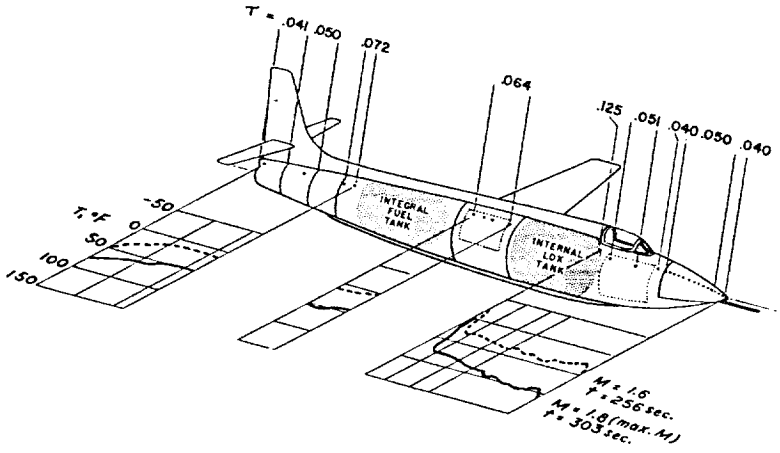

Figure 8

MEASURED TEMPERATURES AT DIFFERENT STATIONS X-1B AIRPLANE

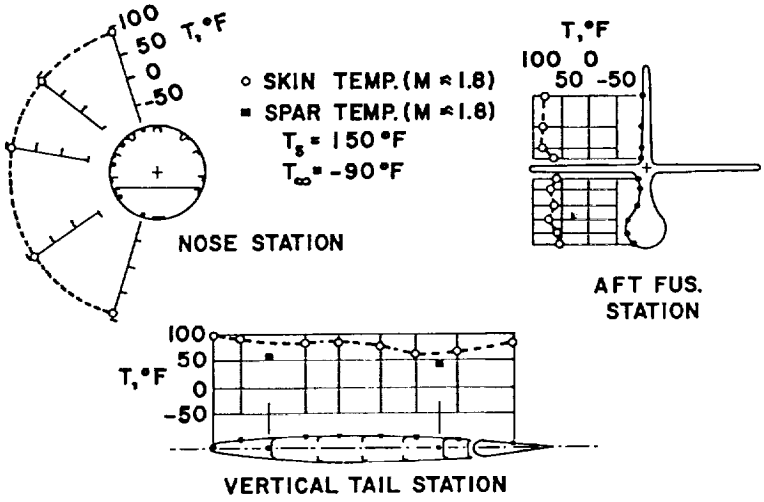

Figure 9

CHORDWISE SKIN TEMPERATURES, X-1B WING

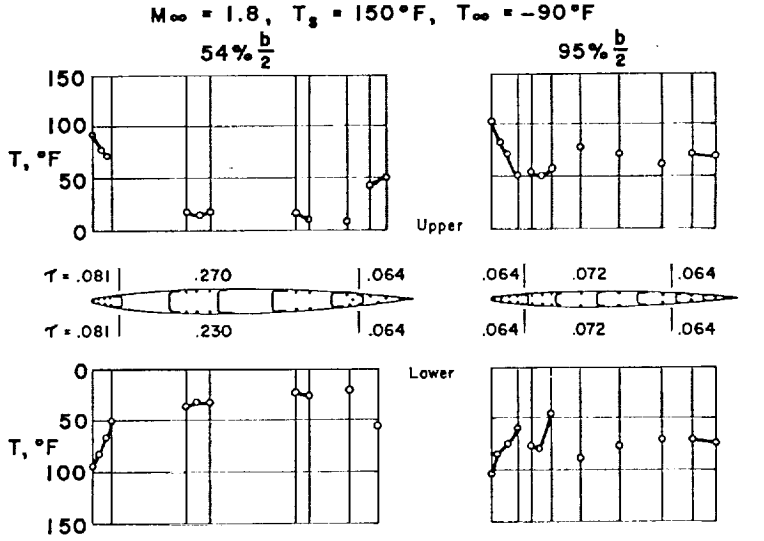

Figure 10

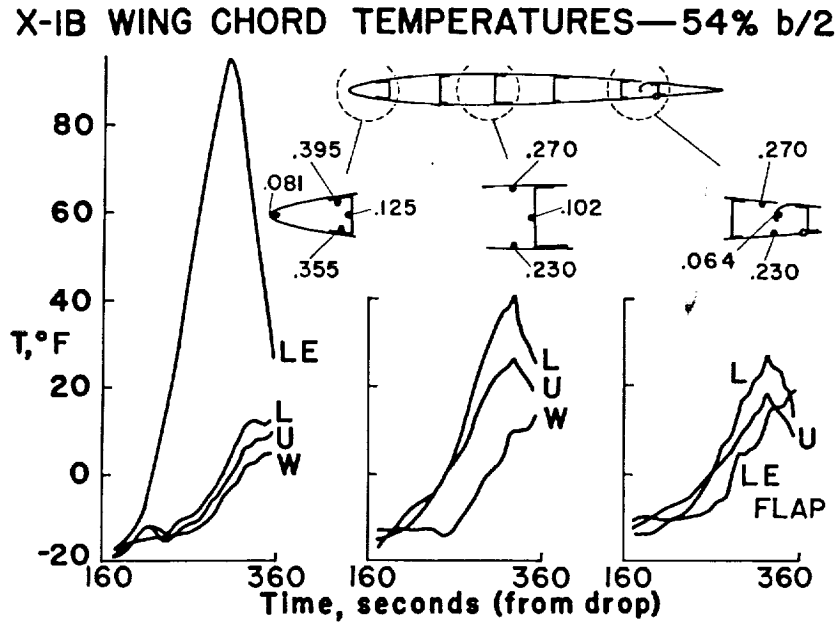

Figure 11

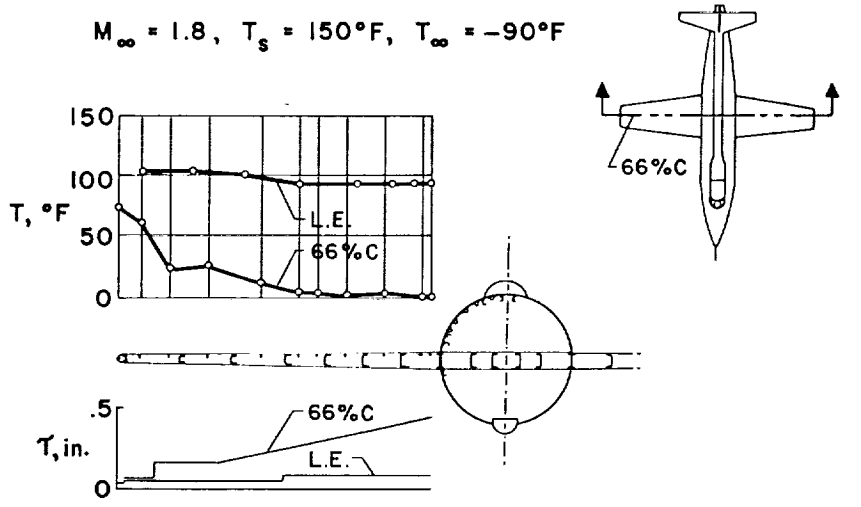

Figure 12